fractal and fractional

MDPI

Article

Dynamics in a Fractional-Order Competitive–Competitive–Cooperative System with Beddington–DeAngelis Functional Responses and Delay

Ting Zhou and Ahmadjan Muhammadhaji *

College of Mathematics and System Sciences, Xinjiang University, Urumqi 830017, China; 107552400685@stu.xju.edu.cn

* Correspondence: ahmatjanam@aliyun.com

Abstract

This study investigates the dynamics of a delayed fractional-order competition-competition-cooperative system with Beddington–DeAngelis functional responses. First, we prove the boundedness and uniqueness of the solutions. We analyze the existence conditions and local asymptotic stability of various equilibrium points using the stability theory. Second, by taking the competition time delay τ as the bifurcation parameter, we derive explicit criteria for the stability of the system and the onset of aHopf bifurcation. Once the delay surpasses a critical threshold, the system loses its stability and displays periodic oscillatory behavior. Furthermore, the influence of the fractional order on the system dynamics is also examined. Finally, numerical simulations are performed to verify the theoretical results, providing significant insights into ecosystem complexity.

Keywords: fractional-order; delay; Hopf bifurcation; Beddington–DeAngelis functional response; stability

1. Introduction

The interactions among biological species are a central topic in the field of ecology. Competition and cooperation are two basic and common types of such interactions. In 1798, Malthus proposed a differential equation model for population growth in his book "An Essay on the Principle of Population". However, this model had a weakness: in reality, no population can grow without limits, because resources are finite. A total of 40 years later, Verhulst improved this model and introduced the logistic model, which better describes the real population growth. In the 1920s, the models introduced by Lotka [1] and Volterra [2] established a theoretical foundation for interspecific interactions. These interactions are commonly modeled as competition, cooperation, parasitism, and predator-prey dynamics. Later, additional factors were added to this model, such as ratio dependence [3], functional responses [4,5], the Allee effect [6], and prey refuge [3,7], either in combination or separately.

However, most classical models only consider one type of interaction at a time. Pure competition often leads to competitive exclusion or weak coexistence with limited resources [8]. The competitive–competitive–cooperative structure is an ecologically vital module, describing two species competing for resources while both cooperating with a third, niche-dependent species. This pattern is exemplified by grass species competing yet sharing mycorrhizal fungi, or bacteria competing while relying on cellulose-degrading actinomycetes. Such mixed interactions stabilize ecosystems, making the competitive–competitive–cooperative model essential for studying species coexistence and community

Check for updates

Academic Editor: Ruihong Li

Received: 3 February 2026
Revised: 2 March 2026
Accepted: 6 March 2026
Published: 8 March 2026

Copyright: © 2026 by the authors. Licensee MDPI, Basel, Switzerland. This article is an open access article distributed under the terms and conditions of the Creative Commons Attribution (CC BY) license.

resilience. Recently, researchers have focused more on extended models that combine multiple interaction types [9–11]. For instance, in 2010, Lv et al. [12] studied the existence and global attractiveness of periodic solutions to a competitor–competitor–mutualist Lotka–Volterra system with deviating arguments. In 2019, Wang et al. [13] investigated the dynamic behavior of a class of three-species of Lotka–Volterra models with feedback controls and time delays. However, the effects of nonlinear functional responses on the population dynamics were not considered in this study. Hence, in 2021, Muhammadhaji et al. [14] studied the dynamic behavior of a ratio-dependent Lotka–Volterra competitive–competitive–cooperative system. Ratio-dependent models can produce unrealistic dynamics where competition or cooperation remains strong, even at low densities. The present study employs the Beddington–DeAngelis functional response to avoid this.

Time delays are widespread in ecological environments, particularly in biological systems. Owing to factors such as gestation, incubation, migration, and resource regeneration [15–17], time delays are often unavoidable. In competitive and cooperative models, delays may arise from the time required for juveniles to mature into adults capable of effective resource competition, or from lags in the realization of benefits in cooperative interactions. Analysis indicates that time delays significantly influence the dynamics of ecological systems and may induce complex dynamic phenomena. Time delays can disrupt or promote the stability of ecosystem dynamics [18]. Therefore, it is both theoretically and practically essential to account for the effects of time delays on ecological dynamic behavior.

Recently, fractional calculus has garnered increasing attention owing to its broad applications across various scientific and engineering disciplines. It has been successfully applied in fields such as systems physics [19,20], finance [21,22], chemistry [23], and biology [24–27]. Studies have revealed that, compared with traditional integer-order systems, fractional-order systems offer advantages such as long-term memory, long-range spatial interactions, and hereditary properties. These features allow fractional-order models to describe dynamic processes with nonlocal characteristics more accurately [28,29]. Berkal et al. [30] highlighted that fractional-order models naturally align with the fractal structures found in biological systems, making them powerful tools for studying complex interactions within ecosystems. Therefore, the use of fractional differential equations is expected to offer deeper insights into the dynamic behaviors and underlying mechanisms of ecological systems.

The phenomenon of Hopf bifurcation has been extensively studied under the classical framework of integer-order delay differential equations, and systematic theoretical analysis methods have been established [31–33]. These investigations have illuminated the manner in which time delays modulate the stability of a system and trigger the generation of periodic solutions when the delay reaches critical values. However, analytical methods for Hopf bifurcation in integer-order models cannot be directly extended to fractional-order differential systems, owing to the nonlocality and memory effects inherent in fractional calculus. Recently, researchers have begun to focus on the Hopf bifurcation in fractional-order delay systems. For instance, Huang et al. [34] explored the stability and bifurcation of a Caputo fractional-order BAM neural network using the time delay and inertia terms. Li et al. [35] constructed a novel fractionally delayed genetic regulatory model and derived sufficient conditions.

Despite these significant advances, most studies have focused on integer-order, competitive, and cooperative systems. However, bifurcation phenomena induced by fractional-order nonlinear dependencies in competitive and cooperative systems have not been systematically investigated. In both competition and cooperation, species dynamics often depend on multiple nonlinear factors, such as resource ratios and individual interference.

Traditional density-dependent models are often inadequate for capturing such nonlinear dependencies. Therefore, Hopf bifurcation behavior in delayed fractional-order nonlinear models within competitive–cooperative systems remains an open problem.

This paper is structured as follows: Section 2 presents the model formulation. Section 3 elaborates on the basic definitions associated with fractional order. In Section 4, we explore the existence and boundedness of solutions to the model. Section 5 is devoted to analyzing the local stability of the system at various equilibrium points. Section 6 conducts the Hopf bifurcation analysis. Numerical simulations are provided in Section 7 to validate our theoretical findings. Finally, Section 8 summarizes the main conclusions derived from this study.

2. The Model Description

In [12], the researchers explored the following time-delayed competitor–competitor–mutualist Lotka–Volterra system:

$$\begin{aligned}
\dot{N}_1(s) &= N_1(s)[c_1(s) - d_{11}(s)N_1(s-\tau_{11}(s)) - d_{12}(s)N_2(s-\tau_{12}(s)) \\
&\quad + d_{13}(s)N_3(s-\tau_{13}(s))], \\
\dot{N}_2(s) &= N_2(s)[c_2(s) - d_{21}(s)N_1(s-\tau_{21}(s)) - d_{22}(s)N_2(s-\tau_{22}(s)) \\
&\quad + d_{23}(s)N_3(s-\tau_{23}(s))], \\
\dot{N}_3(s) &= N_3(s)[c_3(s) + d_{31}(s)N_1(s-\tau_{31}(s)) + d_{32}(s)N_2(s-\tau_{32}(s)) \\
&\quad - d_{33}(s)N_3(s-\tau_{33}(s))],
\end{aligned} \tag{1}$$

where $N_1(s)$ and $N_2(s)$ represent the densities of the competing species at time s, and $N_3(s)$ denotes that of the cooperative species at the same time. In [12], the authors established sufficient conditions for the existence and global attractivity of positive periodic solutions to system (1). In [13], the researchers explored a delayed three-species Lotka–Volterra competitive–cooperative model:

$$\begin{aligned}
\dot{N}_1(s) &= N_1(s)\Big[c_1(s) - d_{11}^1(s)N_1(s-\tau) - d_{11}^2(s)N_1(s-2\tau) - d_{12}(s)N_2(s-2\tau) \\
&\quad + d_{13}(s)N_3(s-\tau) - m_1(s)u_1(s)], \\
\dot{N}_2(s) &= N_2(s)\Big[c_2(s) - d_{21}(s)N_1(s-2\tau) - d_{22}^1(s)N_2(s-\tau) - d_{22}^2(s)N_2(s-2\tau) \\
&\quad + d_{23}(s)N_3(s-\tau) + m_2(s)u_2(s)], \\
\dot{N}_3(s) &= N_3(s)\Big[c_3(s) + d_{31}(s)N_1(s-\tau) + d_{32}(s)N_2(s-\tau) - d_{33}^1(s)N_3(s) \\
&\quad - a_{33}^2(s)N_3(s-\tau) + m_3(s)u_3(s)\Big], \\
\dot{u}_1(s) &= e_1(s) - f_1(s)u_1(s) + q_1(s)N_1(s), \\
\dot{u}_2(s) &= e_2(s) - f_2(s)u_2(s) - q_2(s)N_2(s), \\
\dot{u}_3(s) &= e_3(s) - f_3(s)u_3(s) - q_3(s)N_3(s),
\end{aligned} \tag{2}$$

where $N_i(s)$ $(i = 1, 2, 3)$ denotes the density of each species at time s, and τ is a positive constant. In this work, the permanence and global attractivity of positive solutions to the system are discussed. However, this study did not account for the nonlinear functional

responses among species. Consequently, in 2021, the authors extended system (2) to the following form:

$$\begin{aligned}
\dot{N}_1(s) &= N_1(s)\Big[k_1(s) - a_1(s)N_1(s) - \frac{b_1(s)N_2(s-\tau_1)}{c_1(s)N_2(s-\tau_1)+N_1(s-\tau_1)} \\
&\quad + \frac{d_1(s)N_3(s-\tau_1)}{e_1(s)N_3(s-\tau_1)+N_1(s-\tau_1)} - f_1(s)M_1(s)\Big], \\
\dot{N}_2(s) &= N_2(s)\Big[k_2(s) - a_2(s)N_2(s) - \frac{b_2(s)N_1(s-\tau_2)}{c_2(s)N_1(s-\tau_2)+N_2(s-\tau_2)} \\
&\quad + \frac{d_2(s)N_3(s-\tau_2)}{e_2(s)N_3(s-\tau_2)+N_2(s-\tau_2)} + f_2(s)M_2(s)\Big], \\
\dot{N}_3(s) &= N_3(s)\Big[k_3(s) - a_3(s)N_3(s) + \frac{g_1(s)N_1(s-\tau_3)}{e_1(s)N_3(s-\tau_3)+N_1(s-\tau_3)} \\
&\quad + \frac{g_2(s)N_2(s-\tau_3)}{e_2(s)N_3(s-\tau_3)+N_2(s-\tau_3)} + f_3(s)M_3(s)\Big], \\
\dot{M}_1(s) &= q_1(s) - p_1(s)M_1(s) + h_1(s)N_1(s), \\
\dot{M}_2(s) &= q_2(s) - p_2(s)M_2(s) - h_2(s)N_2(s), \\
\dot{M}_3(s) &= q_3(s) - p_3(s)M_3(s) - h_3(s)N_3(s).
\end{aligned} \tag{3}$$

They derived several sufficient conditions pertaining to the permanence, existence of periodic solutions, and global attractivity of system (3). Nevertheless, previous studies have been predominantly confined to integer-order differential equations.

Inspired by the aforementioned analysis, we propose a fractional-order competitive–cooperative model incorporating Beddington–DeAngelis functional responses, formulated as follows:

$$\begin{aligned}
{}^{c}D_t^{\xi}x_1(t) &= x_1(t)\Big[r_1 - a_1x_1(t) - \tfrac{b_1x_2(t-\tau)}{1+c_1x_2(t-\tau)+x_1(t-\tau)} + \varphi_1x_3(t)\Big], \\
{}^{c}D_t^{\xi}x_2(t) &= x_2(t)\Big[r_2 - a_2x_2(t) - \tfrac{b_2x_1(t-\tau)}{1+c_2x_1(t-\tau)+x_2(t-\tau)} + \varphi_2x_3(t)\Big], \\
{}^{c}D_t^{\xi}x_3(t) &= x_3(t)[r_3 - a_3x_3(t) + \varphi_3x_1(t) + \varphi_4x_2(t)],
\end{aligned} \tag{4}$$

subject to the initial conditions $x_1(\theta) > 0$, $x_2(\theta) > 0$, $x_3(\theta) > 0$, for $\theta \in [-\tau, 0]$.

The Beddington–DeAngelis functional response extends Holling-type responses with interspecific interference terms c_1, c_2, enabling realistic descriptions of species resource utilization in natural ecosystems. Distinct from density-dependent competition models, c_1, c_2 characterize the mutual interference of competing species x_1, x_2 in competition, with their values dictating the saturation rate of the competitive functional response and precisely capturing the nonlinear interspecific competition in the competitive–competitive–cooperative system.

The biological interpretations of the parameters in system (4) are summarized in Table 1.

Remark 1. *In system (4), time delay is introduced only in the competition terms. τ reflects the lag in resource consumption and metabolic feedback between populations. In contrast, cooperative interactions are usually treated as instantaneous because their benefits (e.g., enhanced defense or growth) directly affect current growth rates. This paper focuses on the effect of competitive delay on system stability; hence, delay in cooperation is not considered.*

Table 1. Biological interpretations of the parameters in system (4).

Parameter	Biological Interpretation
$x_1(t)$	The population density of species x_1 at time t.
$x_2(t)$	The population density of species x_2 at time t.
$x_3(t)$	The population density of species x_3 at time t.
r_1, r_2, r_3	The intrinsic growth rates of x_1, x_2, and x_3 respectively.
a_1, a_2, a_3	The intra-specific competition coefficients of x_1, x_2, and x_3 respectively.
b_1	The inter-specific competition coefficient of x_2 on x_1.
b_2	The inter-specific competition coefficient of x_1 on x_2.
c_1, c_2	Saturation constants and quantify interspecific interference intensity during resource competition.
φ_1	The cooperative coefficient of x_3 on x_1.
φ_2	The cooperative coefficient of x_3 on x_2.
φ_3	The cooperative coefficient of x_1 on x_3.
φ_4	The cooperative coefficient of x_2 on x_3.
τ	The time delay generated by competition.

3. Preliminaries

Definition 1 ([36]). *For $t > 0$, the fractional-order integral of order $\xi \in \mathbb{R}_+$ of a function $f(t)$ is defined as:*

$$I_t^{\xi} f(t) = \int_0^t \frac{(t-\tau)^{\xi-1}}{\Gamma(\xi)} f(\tau) d\tau,$$

where $\Gamma(\cdot)$ denotes the Euler gamma function, which is defined as $\Gamma(s) = \int_0^{+\infty} t^{s-1} e^{-t} dt$.

Fractional calculus generalizes integer-order derivatives and integrals to non-integer orders, critical for memory-dependent systems. In this work, we employ the Caputo fractional derivative, which is defined below.

Definition 2 ([36]). *The Caputo fractional-order derivative can be defined in the following form:*

$${}^{c}D_t^{\xi} f(t) = \frac{1}{\Gamma(n-\xi)} \int_0^t (t-\tau)^{n-\xi-1} f^{(n)}(\tau) d\tau,$$

where $n-1 < \xi < n, n \in \mathbb{Z}^+$. In the case when $0 < \xi < 1$, the Caputo fractional-order derivative simplifies to: ${}^{c}D_t^{\xi} f(t) = \frac{1}{\Gamma(1-\xi)} \int_0^t \frac{f'(\tau)}{(t-\tau)^{\xi}} d\tau$.

The Caputo-Fabrizio fractional integral, a non-singular integral, is key to the Hermite-Hadamard type inequality for non-convex functions-this inequality provides integral bounds and lays the theoretical foundation for our fractional-order system analysis.

Definition 3 ([37]). *The Laplace transform of the Caputo fractional-order derivatives is defined as follows:*

$$\mathcal{L}\{{}^{c}D_t^{\xi} f(t); s\} = s^{\xi} \mathcal{F}(s) - \sum_{i=0}^{n-1} s^{\xi-i-1} f^{(i)}(0),$$

where $\mathcal{F}(s) = \mathcal{L}\{f(t)\}$, which means the Laplace transform of $f(t)$. Additionally, when $f^{(i)}(0) = 0, (i = 0, 1, \ldots, n-1)$, it satisfies $\mathcal{L}\{{}^{c}D_t^{\xi} f(t); s\} = s^{\xi} \mathcal{F}(s)$.

Lemma 1 ([37]). *Consider the following Caputo fractional-order system:*

$${}^{c}D_t^{\xi} \boldsymbol{x}(t) = \boldsymbol{f}(t, \boldsymbol{x}(t)), \quad \boldsymbol{x}(0) = \boldsymbol{x}_0,$$

in which $\boldsymbol{f}(t, \boldsymbol{x}(t))$ is an n-dimensional real-valued continuous vector function with $0 < \xi \leq 1$ and $\boldsymbol{x} \in R^n$. The equilibrium points of the above system are calculated by solving the following

equation: $\boldsymbol{f}(t, \boldsymbol{x}(t)) = 0$, *where* $\boldsymbol{f} = [f_1,\ f_2,\ \ldots,\ f_n]^T$. *These points are locally asymptotically stable if all eigenvalues* λ_i *of the Jacobian matrix* $J = \frac{\partial f}{\partial x}$ *evaluated at the equilibrium points satisfy:* $|\arg(\lambda_i)| > \frac{\xi\pi}{2}$. *Otherwise, the equilibrium point is unstable.*

Lemma 2 ([38]). *Suppose that* $f(t)$ *is a continuous function defined on the interval* $[0, +\infty)$ *and fulfills the following condition(s):*

$$\begin{cases} {}^cD_t^{\xi} f(t) + \iota f(t) \leqslant \kappa, \\ f(0) = \kappa_0, \end{cases}$$

where $0 < \xi < 1, (\iota, \kappa) \in R^2$ *and* $\iota > 0$, *one has*

$$f(t) \leq \{f(0) - \frac{\kappa}{\iota}\} E_{\xi,1}\{-\iota t^{\xi}\} + \frac{\kappa}{\iota}.$$

Considering the following n-dimensional fractional-order system with multiple time delays [39]:

$$\begin{cases} {}^cD_t^{\xi_1} x_1(t) = a_{11}x_1(t-\tau_{11}) + a_{12}x_2(t-\tau_{12}) + \cdots + a_{1n}x_n(t-\tau_{1n}), \\ {}^cD_t^{\xi_2} x_2(t) = a_{21}x_1(t-\tau_{21}) + a_{22}x_2(t-\tau_{22}) + \cdots + a_{2n}x_n(t-\tau_{2n}), \\ \vdots \\ {}^cD_t^{\xi_n} x_n(t) = a_{n1}x_1(t-\tau_{n1}) + a_{n2}x_2(t-\tau_{n2}) + \cdots + a_{nn}x_n(t-\tau_{nn}), \end{cases} \tag{5}$$

where $\xi_i \in (0, 1], i = 1, 2, \ldots, n$, $\tau_{\max} = \max_{1 \leq i,j \leq n}\{\tau_{ij}\}$ *and* $-\tau_{\max} \leq t \leq 0, i = 1, 2, \ldots, n$. *The corresponding characteristic equation of system* (5) *is defined as:*

$$\det \begin{pmatrix} s^{\xi_1} - a_{11}e^{-s\tau_{11}} & -a_{12}e^{-s\tau_{12}} & \cdots & -a_{1n}e^{-s\tau_{1n}} \\ -a_{21}e^{-s\tau_{21}} & s^{\xi_2} - a_{22}e^{-s\tau_{22}} & \cdots & -a_{2n}e^{-s\tau_{2n}} \\ \vdots & \vdots & \ddots & \vdots \\ -a_{n1}e^{-s\tau_{n1}} & -a_{n2}e^{-s\tau_{n2}} & \cdots & s^{\xi_n} - a_{nn}e^{-s\tau_{nn}} \end{pmatrix} = 0.$$

4. Existence and Uniform Boundness

Theorem 1. *For any non-negative initial condition, system* (4) *has a unique solution for in* $\Pi = \{\boldsymbol{x} = (x_1, x_2, x_3) \in \mathbb{R}^3, \max\{|x_1|, |x_2|, |x_3| \leq M\}\}$.

Proof. To prove the theorem, we introduce a mapping

$$\boldsymbol{f}(\boldsymbol{x}) = (f_1(\boldsymbol{x}), f_2(\boldsymbol{x}), f_3(\boldsymbol{x})),$$

where $\boldsymbol{x} = (x_1, x_2, x_3)$, $\hat{\boldsymbol{x}} = (\hat{x}_1, \hat{x}_2, \hat{x}_3)$ and

$$\begin{aligned} f_1(\boldsymbol{x}) &= x_1(t)\Big[r_1 - a_1x_1(t) - \tfrac{b_1x_2(t-\tau)}{1+c_1x_2(t-\tau)+x_1(t-\tau)} + \varphi_1x_3(t)\Big], \\ f_2(\boldsymbol{x}) &= x_2(t)\Big[r_2 - a_2x_2(t) - \tfrac{b_2x_1(t-\tau)}{1+c_2x_1(t-\tau)+x_2(t-\tau)} + \varphi_2x_3(t)\Big], \\ f_3(\boldsymbol{x}) &= x_3(t)[r_3 - a_3x_3(t) + \varphi_3x_1(t) + \varphi_4x_2(t)]. \end{aligned}$$

For any $\boldsymbol{x}, \hat{\boldsymbol{x}} \in \Pi$, we have

$$\begin{aligned}
& \|\boldsymbol{f}(\boldsymbol{x}) - \boldsymbol{f}(\hat{\boldsymbol{x}})\| \\
= \; & \textstyle\sum_{i=1}^{3} |f_i(\boldsymbol{x}) - f_i(\hat{\boldsymbol{x}})| \\
= \; & \Big| x_1(t)\Big[r_1 - a_1 x_1(t) - \tfrac{b_1 x_2(t-\tau)}{1+c_1 x_2(t-\tau)+x_1(t-\tau)} + \varphi_1 x_3(t)\Big] \\
& - \Big\{ \hat{x}_1(t)\Big[r_1 - a_1 \hat{x}_1(t) - \tfrac{b_1 \hat{x}_2(t-\tau)}{1+c_1 \hat{x}_2(t-\tau)+\hat{x}_1(t-\tau)} + \varphi_1 \hat{x}_3(t)\Big] \Big\} \Big| \\
& + \Big| x_2(t)\Big[r_2 - a_2 x_2(t) - \tfrac{b_2 x_1(t-\tau)}{1+c_2 x_1(t-\tau)+x_2(t-\tau)} + \varphi_2 x_3(t)\Big] \\
& - \Big\{ \hat{x}_2(t)\Big[r_2 - a_2 \hat{x}_2(t) - \tfrac{b_2 \hat{x}_1(t-\tau)}{1+c_2 \hat{x}_1(t-\tau)+\hat{x}_2(t-\tau)} + \varphi_2 \hat{x}_3(t)\Big] \Big\} \Big| \\
& + |x_3(t)[r_3 - a_3 x_3(t) + \varphi_3 x_1(t) + \varphi_4 x_2(t)] \\
& - \{x_3(t)[r_3 - a_3 x_3(t) + \varphi_3 x_1(t) + \varphi_4 x_2(t)]\}| \\
\leq \; & \Big(r_1 + 2a_1 M + \tfrac{c_1 b_1 + 2b_1 M^2}{{c_1}^2} + \varphi_1 M + \tfrac{2b_2 M^2}{{c_2}^2} + \varphi_3 M\Big)|x_1(t) - \hat{x}_1(t)| \\
& + \Big(\tfrac{2b_1 M^2}{{c_1}^2} + r_2 + 2a_2 M + \tfrac{c_2 b_2 + 2b_2 M^2}{{c_2}^2} + \varphi_2 M + \varphi_4 M\Big)|x_2(t) - \hat{x}_2(t)| \\
& + \{r_3 + (\varphi_1 + \varphi_2 + \varphi_3 + \varphi_4)M\}|x_3(t) - \hat{x}_3(t)| \\
\leq \; & L \parallel \boldsymbol{x} - \hat{\boldsymbol{x}} \parallel,
\end{aligned}$$

where $L = \max\{r_1 + 2a_1 M + \frac{c_1 b_1 + 2b_1 M^2}{{c_1}^2} + \varphi_1 M + \frac{2b_2 M^2}{{c_2}^2} + \varphi_3 M, \frac{2b_1 M^2}{{c_1}^2} + r_2 + 2a_2 M + \frac{c_2 b_2 + 2b_2 M^2}{{c_2}^2} + \varphi_2 M + \varphi_4 M, r_3 + (\varphi_1 + \varphi_2 + \varphi_3 + \varphi_4)M\}$. Therefore, $f(x)$ satisfies the local Lipschitz condition and proves system (4) has a unique solution $x(t)$. □

Theorem 2. *If $\mu_i > 0$ $(i = 1,2,3)$, then any solution of system (4) with initial conditions $x_1(\theta) > 0$, $x_2(\theta) > 0$, $x_3(\theta) > 0$, for $\theta \in [-\tau, 0]$ remains uniformly bounded in the region Γ, where μ_i $(i = 1,2,3)$ will be defined in the proof and*

$$\Gamma = \left\{ (x_1, x_2, x_3) \in \mathbb{R}^3_+ : V(t) \leq \frac{3(r+\lambda)^2}{4\mu\lambda} + \varrho, \varrho > 0 \right\}.$$

Proof. Let us consider the function $V(t) = x_1(t) + x_2(t) + x_3(t)$. Then we have

$$\begin{aligned}
D^{\xi} V(t) = \; & D^{\xi} x_1(t) + D^{\xi} x_2(t) + D^{\xi} x_3(t) \\
= \; & x_1\Big[r_1 - a_1 x_1 - \tfrac{b_1 x_2}{1+c_1 x_2 + x_1} + \varphi_1 x_3\Big] \\
& + x_2\Big[r_2 - a_2 x_2 - \tfrac{b_2 x_1}{1+c_2 x_1 + x_2} + \varphi_2 x_3\Big] \\
& + x_3[r_3 - a_3 x_3 + \varphi_3 x_1 + \varphi_4 x_2] \\
\leq \; & r_1 x_1 + r_2 x_2 + r_3 x_3 - \mu_1 {x_1}^2 - \mu_2 {x_2}^2 - \mu_3 {x_3}^2,
\end{aligned}$$

where $\mu_1 = a_1 - \frac{\varphi_1 + \varphi_3}{2}, \mu_2 = a_2 - \frac{\varphi_2 + \varphi_4}{2}, \mu_3 = a_3 - \frac{\varphi_1 + \varphi 2 + \varphi_3 + \varphi 4}{2}$. Now, we consider a real number $\lambda > 0$. Thus,

$$\begin{aligned}
D^{\xi} V(t) + \lambda V(t) \leq \; & (r_1 + \lambda)x_1 - \mu_1 {x_1}^2 + (r_2 + \lambda)x_2 - \mu_2 {x_2}^2 + (r_3 + \lambda)x_3 - \mu_3 {x_3}^2 \\
\leq \; & \tfrac{(r_1+\lambda)^2}{4\mu_1} + \tfrac{(r_2+\lambda)^2}{4\mu_2} + \tfrac{(r_3+\lambda)^2}{4\mu_3}.
\end{aligned}$$

If $\mu_1, \mu_2, \mu_3 > 0$, $r = \max\{r_1, r_2, r_3\}$ and $\mu = \min\{\mu_1, \mu_2, \mu_3\}$. Then, from the above formula, we obtain

$$D^{\xi} V(t) + \lambda V(t) \leq \frac{3(r+\lambda)^2}{4\mu} = G.$$

Applying Lemma 2 to our inequality with $\iota = \lambda$ and $\kappa = G$, we obtain

$$V(t) \leq V(0) E_{\xi,1}(-\lambda t^{\xi}) - \frac{G}{\lambda} E_{\xi,1}(-\lambda t^{\xi}) + \frac{G}{\lambda},$$

where $E_{\xi,1}(.)$ is the two-parameter Mittag-Leffler function. Since the Mittag-Leffler function $E_{\xi,1}(-\lambda t^{\xi}) \to 0$ as $t \to \infty$ for $\lambda > 0$ and $0 < \xi < 1$, then we obtain

$$V(t) \leq \frac{G}{\lambda} = \frac{3(r+\lambda)^2}{4\mu\lambda}, \quad \text{as} \quad t \to \infty.$$

Therefore, any solution of system (4) initiating from an interior point of $\mathbb{R}^3_+$ is uniformly bounded in

$$\Gamma = \left\{ (x_1, x_2, x_3) \in \mathbb{R}^3_+ : V(t) \leq \frac{3(r+\lambda)^2}{4\mu\lambda} + \varrho, \varrho > 0 \right\}.$$

□

5. Local Stability of Equilibrium Points

We now analyze the steady states of the proposed system (4). By definition, a steady state corresponds to a constant solution of the system, which is also referred to as an equilibrium point. In this section, we investigate the biologically feasible equilibria of system (4) and assess their stability characteristics. The equilibrium points of system (4) are derived as follows:

(i) The trivial equilibrium point $E_0 = (0, 0, 0)$ always exists.
(ii) The axial equilibrium point $E_1 = (\tilde{x}_1, 0, 0)$ exists with $\tilde{x}_1 = \frac{r_1}{a_1}$, and is independent of the parameters.
(iii) The planar equilibrium point $E_2 = (\ddot{x}_1, 0, \ddot{x}_3)$ exists if $a_1 a_3 > \varphi_1 \varphi_3$, where

$$\ddot{x}_1 = \frac{r_1 a_3 + \varphi_1 r_3}{a_1 a_3 - \varphi_1 \varphi_3}, \ \ddot{x}_3 = \frac{r_3 a_1 + \varphi_3 r_1}{a_1 a_3 - \varphi_1 \varphi_3}.$$

(iv) $E_3 = (x_1^*, x_2^*, x_3^*)$ is the positive equilibrium point, if the following conditions:

$$\begin{aligned} r_1 - a_1 x_1^* - \tfrac{b_1 x_2^*}{1 + c_1 x_2^* + x_1^*} + \varphi_1 x_3^* &= 0, \\ r_2 - a_2 x_2^* - \tfrac{b_2 x_1^*}{1 + c_2 x_1^* + x_2^*} + \varphi_2 x_3^* &= 0, \\ r_3 - a_3 x_3^* + \varphi_3 x_1^* + \varphi_4 x_2^* &= 0. \end{aligned}$$

Solving the third equation of the above system for x_3^*, we can obtain $x_3^* = m_1 + m_2 x_1^* + m_3 x_2^*$, where $m_1 = \frac{r_3}{a_3}, m_2 = \frac{\varphi_3}{a_3}, m_3 = \frac{\varphi_4}{a_3}$.
Substituting x_3^* into the first two equations yields:

$$\begin{aligned} d_1 + d_2 x_1^* + d_3 x_2^* &= \frac{b_1 x_2^*}{1 + c_1 x_2^* + x_1^*}, \\ e_1 + e_2 x_1^* + e_3 x_2^* &= \frac{b_2 x_1^*}{1 + c_2 x_1^* + x_2^*}, \end{aligned}$$

where

$$\begin{aligned} d_1 = r_1 + \varphi_1 m_1, d_2 = \varphi_1 m_2 - a_1, d_3 = \varphi_1 m_3, \\ e_1 = r_2 + \varphi_2 m_1, e_2 = \varphi_2 m_2, e_3 = \varphi_2 m_3 - a_2. \end{aligned}$$

Given the difficulty in analytically determining x_1^* and x_2^*, we verify their existence via numerical simulations, as illustrated in Figure 1.

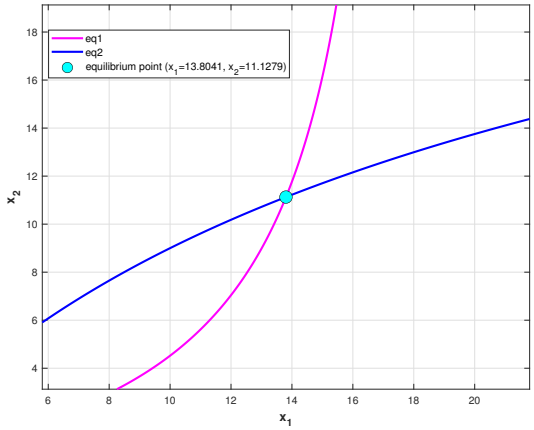


Figure 1. The unique intersection point at (x_1^*, x_2^*) demonstrates stable coexistence of both populations.

Although the closed-form solutions of x_1^* and x_2^* are intractable, the existence and uniqueness of the positive equilibrium $E_3 = (x_1^*, x_2^*, x_3^*)$ can be theoretically guaranteed by Krasnoselskii's fixed-point theorem for compact operators on convex closed sets in $\mathbb{R}^2_+$ [40]. Let the mapping $F : (x_1, x_2) \to (F_1(x_1, x_2), F_2(x_1, x_2))$ be defined by the implicit equations of E_3 after substituting $x_3^* = m_1 + m_2 x_1 + m_3 x_2$. Under the conditions that all model parameters $(r_i > 0, a_i > 0, b_i > 0, \varphi_i > 0, c_i > 0)$ are strictly positive and the boundedness of the Beddington–DeAngelis functional response (ensuring F is bounded and continuous), F is a compact mapping on a sufficiently large convex closed set $K \in \mathbb{R}^2_+$. By Krasnoselskii's theorem, F has at least one fixed point in K, corresponding to a positive (x_1^*, x_2^*). For uniqueness, the algebraic resultant method [41] can be applied to eliminate variables from the implicit equations, yielding a univariate polynomial whose simple positive real root (guaranteed by the model's ecological parameter constraints) ensures a unique positive (x_1^*, x_2^*). Numerical simulation (Figure 1) further validates this theoretical result and gives the explicit coordinate of E_3.

Since, $r_3, a_3, \varphi_3, \varphi_4 > 0$, we have $m_1 = \frac{r_3}{a_3} > 0, m_2 = \frac{\varphi_3}{a_3} > 0, m_3 = \frac{\varphi_4}{a_3} > 0$. Thus, the condition $m_1 + m_2 x_1^* + m_3 x_2^* > 0$ is automatically satisfied. Hence, the positive equilibrium E_3 exists.

Theorem 3. *The trivial equilibrium point $E_0 = (0, 0, 0)$ is unstable.*

Proof. The eigenvalues of the $J(E_0)$ are $\lambda_1 = r_1 > 0, \lambda_2 = r_2 > 0$ and $\lambda_3 = r_3 > 0$. Hence

$$|arg(\lambda_{1,2,3})| = 0 < \frac{\pi\xi}{2}. \tag{6}$$

Based on Lemma 1, the trivial equilibrium point E_0 is unstable. □

Theorem 4. *The axial equilibrium point $E_1 = (\tilde{x}_1, 0, 0)$ is unstable.*

Proof. The Jacobian matrix for system at E_1 is given by

$$J(E_1) = \begin{pmatrix} -r_1 & -\frac{b_1 r_1}{a_1 + r_1} & \frac{\varphi_1 r_1}{a_1} \\ 0 & r_2 - \frac{b_2 r_1}{a_1 + c_2 r_1} & 0 \\ 0 & 0 & r_3 + \frac{\varphi_3 r_1}{a_1} \end{pmatrix},$$

the characteristic equation of $J(E_1)$ is given by

$$(\lambda + r_1)\left(\lambda - r_2 + \frac{b_2 r_1}{a_1 + c_2 r_1}\right)\left(\lambda - r_3 - \frac{\varphi_3 r_1}{a_1}\right) = 0. \tag{7}$$

Since $r_3 + \frac{\varphi_3 r_1}{a_1} > 0$, Equation (7) possesses one eigenvalue that is a positive real number. By Lemma 1, we can obtain E_1 is unstable. □

Theorem 5. *The planar equilibrium point $E_2 = (\ddot{x}_1, 0, \ddot{x}_3)$ is locally asymptotically stable if one of the following conditions holds:*

(1) $r_2 + \varphi_2 \ddot{x}_3 < \frac{b_2 \ddot{x}_1}{1 + c_2 \ddot{x}_1}, \epsilon_1 \geq 0, \epsilon_0 > 0.$

(2) $r_2 + \varphi_2 \ddot{x}_3 < \frac{b_2 \ddot{x}_1}{1 + c_2 \ddot{x}_1}, \epsilon_1 < 0, \epsilon_1^2 - 4\epsilon_0 < 0, |\tan^{-1}(\frac{\sqrt{4\epsilon_0 - \epsilon_1^2}}{\epsilon_1})| > \frac{\pi\xi}{2}.$

where the parameters ϵ_1 and ϵ_0 are defined in the proof.

Proof. For the system under consideration, the Jacobian matrix corresponding to equilibrium E_2 is presented below:

$$J(E_2) = \begin{pmatrix} \beta_1 & \beta_2 & \beta_3 \\ 0 & \beta_4 & 0 \\ \beta_5 & \beta_6 & \beta_7 \end{pmatrix},$$

where

$$\beta_1 = r_1 - 2a_1\ddot{x}_1 + \varphi_1\ddot{x}_3,\ \beta_2 = -\frac{b_1\ddot{x}_1}{1+\ddot{x}_1},\ \beta_3 = \varphi_1\ddot{x}_1,$$
$$\beta_4 = r_2 - \frac{b_2\ddot{x}_1}{1+c_2\ddot{x}_1} + \varphi_2\ddot{x}_3,\ \beta_5 = \varphi_3\ddot{x}_3,\ \beta_6 = \varphi_4\ddot{x}_3,\ \beta_7 = r_3 - 2a_3\ddot{x}_3 + \varphi_3\ddot{x}_1.$$

For $J(E_2)$, the associated characteristic equation is formulated as below:

$$(\lambda - \beta_4)\{(\lambda - \beta_1)(\lambda - \beta_7) - \beta_3\beta_5\} = 0. \tag{8}$$

Obviously $\lambda_1 = \beta_4$, then $\lambda_1 > 0$ if $r_2 + \varphi_2\ddot{x}_3 > \frac{b_2\ddot{x}_1}{1+c_2\ddot{x}_1}$. See that

$$|arg(\lambda_1)| = 0 < \frac{\pi\xi}{2}. \tag{9}$$

Therefore, regardless of the signs of the other two eigenvalues, E_2 is always unstable. Now, assuming the condition $r_2 + \varphi_2\ddot{x}_3 < \frac{b_2\ddot{x}_1}{1+c_2\ddot{x}_1}$ is satisfied, the remaining two eigenvalues are obtained from solving the following quadratic equation:

$$(\lambda^2 + \epsilon_1\lambda + \epsilon_0) = 0, \tag{10}$$

where $\epsilon_1 = -(\beta_1 + \beta_7),\ \epsilon_0 = \beta_1\beta_7 - \beta_3\beta_5$. By solving (10), we have

$$\lambda_{2,3} = \frac{-\epsilon_1 \pm \sqrt{\epsilon_1^2 - 4\epsilon_0}}{2}. \tag{11}$$

Case I: Assume $\epsilon_1 \geq 0$ and $\epsilon_0 > 0$. There are three sub-cases to consider here.

(a) If $\epsilon_1 = 0$, the roots of Equation (10) are two complex conjugate eigenvalues $\lambda_2 = \sqrt{\epsilon_0}i, \lambda_3 = \overline{\lambda_2}$ and $Re(\lambda_2) = Re(\lambda_3) = 0$. Obviously

$$|arg(\lambda_{2,3})| = \frac{\pi}{2} > \frac{\pi\xi}{2}. \tag{12}$$

(b) If $\epsilon_1 > 0$ and $\epsilon_1^2 - 4\epsilon_0 \geq 0$, then the eigenvalues are negative real values $\lambda_2 < 0$ and $\lambda_3 < 0$. Hence

$$|arg(\lambda_{2,3})| = \pi > \frac{\pi\xi}{2}. \tag{13}$$

(c) If $\epsilon_1 > 0$ and $\epsilon_1^2 - 4\epsilon_0 < 0$, we obtain a pair of complex conjugate eigenvalues $\lambda_2 = -\frac{\epsilon_1}{2} + \frac{\sqrt{4\epsilon_0 - \epsilon_1^2}}{2}i$, $\lambda_3 = \overline{\lambda_2}$ and $Re(\lambda_2) = Re(\lambda_3) < 0$. Then we have

$$|arg(\lambda_{2,3})| > \frac{\pi\xi}{2}. \tag{14}$$

According to Lemma 1, the planar equilibrium point E_2 of system (4) is locally asymptotically stable as $\epsilon_1 \geq 0$ and $\epsilon_0 > 0$. Case II: For the conditions $\epsilon_1 < 0, \epsilon_1^2 - 4\epsilon_0 < 0$ ensure that the eigenvalues are complex numbers with strictly positive real parts. To determine the local stability of E_2, it is also satisfy the last condition $|\tan^{-1}(\frac{\sqrt{4\epsilon_0 - \epsilon_1^2}}{\epsilon_1})| > \frac{\pi\xi}{2}$. We can obtain

$$|arg(\lambda_{2,3})| = |\tan^{-1}(\frac{\sqrt{4\epsilon_0 - \epsilon_1^2}}{\epsilon_1})| > \frac{\pi\xi}{2}. \tag{15}$$

□

6. Hopf Bifurcation

In this section, we aim to establish the thresholds for Hopf bifurcation with time delays employed as bifurcation parameters. For the sake of convenience, we introduce the following transformation:

$$y_1(t) = x_1(t) - x_1^*,\ y_2(t) = x_2(t) - x_2^*,\ y_3(t) = x_3(t) - x_3^*,$$

and system (4) turns into:

$$\begin{aligned}
{}^cD_t^\xi y_1(t) &= (y_1(t) + x_1^*)\Big[r_1 - a_1(y_1(t) + x_1^*) - \frac{b_1(y_2(t-\tau) + x_2^*)}{1 + c_1(y_2(t-\tau) + x_2^*) + (y_1(t-\tau) + x_1^*)} \\
&\quad + \varphi_1(y_3(t) + x_3^*)\Big], \\
{}^cD_t^\xi y_2(t) &= (y_2(t) + x_2^*)\Big[r_2 - a_2(y_2(t) + x_2^*) - \frac{b_2(y_1(t-\tau) + x_1^*)}{1 + c_2(y_1(t-\tau) + x_1^*) + (y_2(t-\tau) + x_2^*)} \\
&\quad + \varphi_2(y_3(t) + x_3^*)\Big], \\
{}^cD_t^\xi y_3(t) &= (y_3(t) + x_3^*)[r_3 - a_3(y_3(t) + x_3^*) + \varphi_3(y_1(t) + x_1^*) \\
&\quad + \varphi_4(y_2(t) + x_2^*)].
\end{aligned} \tag{16}$$

Let $E^* = (x_1^*, x_2^*, x_3^*,)$ be the positive equilibrium of system (16). We linearize the nonlinear vector field around E^* by computing the Jacobian matrix

$$J = (\frac{\partial F_i}{\partial y_j})_{i.j=1,2,3}.$$

Using the structure of the Beddington–DeAngelis functional response and evaluating at E^*, we obtain the partial derivatives step by step:

For the first equation:

$$\frac{\partial F_1}{\partial y_1} = -a_1 x_1^* + \frac{b_1 x_1^* x_2^*}{(1 + c_1 x_2^* + x_1^*)^2}, \quad \frac{\partial F_1}{\partial y_2} = -\frac{b_1(x_1^* + 1)x_1^*}{(1 + c_1 x_2^* + x_1^*)^2}, \quad \frac{\partial F_1}{\partial y_3} = \varphi_1 x_1^*.$$

For the second equation:

$$\frac{\partial F_2}{\partial y_1} = -\frac{b_2(x_2^*+1)x_2^*}{(1+c_2x_1^*+x_2^*)^2}, \quad \frac{\partial F_2}{\partial y_2} = -a_2x_2^* + \frac{b_2x_1^*x_2^*}{(1+c_2x_1^*+x_2^*)^2}, \quad \frac{\partial F_2}{\partial y_3} = \varphi_2x_2^*.$$

For the third equation:

$$\frac{\partial F_3}{\partial y_1} = \varphi_3x_3^*, \quad \frac{\partial F_3}{\partial y_2} = \varphi_4x_3^*, \quad \frac{\partial F_3}{\partial y_3} = -a_3x_3^*.$$

We denote these partial derivatives evaluated at E^* by

$$q_{ij} = \left.\frac{\partial F_i}{\partial y_j}\right|_{E^*}, \quad i,j = 1,2,3.$$

Then the linearized system corresponding to (16) is given by

$$\begin{aligned} {}^cD_t^{\xi}y_1(t) &= q_{11}y_1(t) + q_{12}y_1(t-\tau) + q_{13}y_2(t-\tau) + q_{14}y_3(t), \\ {}^cD_t^{\xi}y_2(t) &= q_{21}y_1(t-\tau) + q_{22}y_2(t) + q_{23}y_2(t-\tau) + q_{24}y_3(t), \\ {}^cD_t^{\xi}y_3(t) &= q_{31}y_1(t) + q_{32}y_2(t) + q_{33}y_3(t), \end{aligned} \tag{17}$$

where each coefficient q_{ij} is explicitly expressed in terms of the equilibrium values x_1^*, x_2^*, x_3^* and model parameters. This completes the transparent derivation of the linearized system. With respect to the Hopf bifurcation of system (17), we first present the following lemma.

Lemma 3. *When $\tau = 0$, if one of the following assumptions is satisfied:*

(H1): $D(p) > 0, \Lambda_1 > 0, \Lambda_3 > 0$ *and* $\Lambda_1\Lambda_2 > \Lambda_3$.
(H2): $D(p) < 0, \Lambda_1 \geq 0, \Lambda_2 \geq 0, \Lambda_3 > 0, \xi < 2/3$.
(H3): $D(p) < 0, \Lambda_1 > 0, \Lambda_2 > 0, \Lambda_1\Lambda_2 = \Lambda_3$ *for all* $\xi \in [0,1)$.

Then the positive equilibrium point $E_3 = (x_1^*, x_2^*, x_3^*)$ is locally asymptotically stable, where $p(\lambda) = \lambda^3 + \Lambda_1\lambda^2 + \Lambda_2\lambda + \Lambda_3$, $D(p)$ is the discriminant of a polynomial $p(\lambda)$,

$$\begin{aligned} D(p) &= -\det\begin{pmatrix} 1 & \Lambda_1 & \Lambda_2 & \Lambda_3 & 0 \\ 0 & 1 & \Lambda_1 & \Lambda_2 & \Lambda_3 \\ 3 & 2\Lambda_1 & \Lambda_2 & 0 & 0 \\ 0 & 3 & 2\Lambda_1 & \Lambda_2 & 0 \\ 0 & 0 & 3 & 2\Lambda_1 & \Lambda_2 \end{pmatrix} \\ &= 18\Lambda_1\Lambda_2\Lambda_3 + (\Lambda_1\Lambda_2)^2 - 4\Lambda_3\Lambda_1^2 - 4\Lambda_2^2 - 27\Lambda_3^2, \end{aligned}$$

and

$$\begin{aligned} \Lambda_1 &= -(q_{11}+q_{12}+q_{22}+q_{23}+q_{33}), \\ \Lambda_2 &= (q_{11}+q_{12})(q_{22}+q_{23}) + (q_{11}+q_{12})q_{33} + (q_{22}+q_{23})q_{33} \\ &\quad - q_{24}q_{32} - q_{13}q_{21} - q_{14}q_{31}, \\ \Lambda_3 &= -(q_{11}+q_{12})(q_{22}+q_{23})q_{33} + (q_{11}+q_{12})q_{24}q_{32} + q_{13}q_{21}q_{33} \\ &\quad - q_{13}q_{24}q_{31} - q_{14}q_{21}q_{32} + q_{14}q_{31}(q_{22}+q_{23}). \end{aligned}$$

Proof. For $\tau = 0$, the coefficient matrix Ψ of system (17) is given by:

$$\Psi = \begin{pmatrix} q_{11}+q_{12} & q_{13} & q_{14} \\ q_{21} & q_{22}+q_{23} & q_{24} \\ q_{31} & q_{32} & q_{33} \end{pmatrix},$$

the characteristic equation is

$$\lambda^3 + \Lambda_1\lambda^2 + \Lambda_2\lambda + \Lambda_3 = 0,$$

If any one of the assumptions (H1–H3) holds, it can be verified via the Routh-Hurwitz criterion that all eigenvalues of system (17) have strictly negative real parts. Consequently, the equilibrium point E_3 is locally asymptotically stable.
Then, by Definition 3, taking Laplace transform in system (17) yields:

$$\begin{cases} s^{\xi}\mathcal{L}[y_1(t)] - s^{\xi-1}\phi_1(0) = q_{11}\mathcal{L}[y_1(t)] + q_{12}e^{-s\tau}\left(\mathcal{L}[y_1(t)] + \int_{-\tau}^{0} e^{-st}\phi_1(t)dt\right) \\ \qquad\qquad + q_{13}e^{-s\tau}\left(\mathcal{L}[y_2(t)] + \int_{-\tau}^{0} e^{-st}\phi_2(t)dt\right) + q_{14}\mathcal{L}[y_3(t)], \\ s^{\xi}\mathcal{L}[y_2(t)] - s^{\xi-1}\phi_2(0) = q_{21}e^{-s\tau}\left(\mathcal{L}[y_1(t)] + \int_{-\tau}^{0} e^{-st}\phi_1(t)dt\right) + q_{22}\mathcal{L}[y_2(t)] \\ \qquad\qquad + q_{23}e^{-s\tau}\left(\mathcal{L}[y_2(t)] + \int_{-\tau}^{0} e^{-st}\phi_2(t)dt\right) + q_{24}\mathcal{L}[y_3(t)], \\ s^{\xi}\mathcal{L}[y_3(t)] - s^{\xi-1}\phi_3(0) = q_{31}\mathcal{L}[y_1(t)] + q_{32}\mathcal{L}[y_2(t)] + q_{33}\mathcal{L}[y_3(t)], \end{cases}$$

which becomes

$$\begin{aligned} s^{\xi}\mathcal{F}_1(s) &= (q_{11} + q_{12}e^{-s\tau})\mathcal{F}_1(s) + q_{13}e^{-s\tau}\mathcal{F}_2(s) + q_{14}\mathcal{F}_3(s), \\ s^{\xi}\mathcal{F}_2(s) &= q_{21}e^{-s\tau}\mathcal{F}_1(s) + (q_{22} + q_{23}e^{-s\tau})\mathcal{F}_2(s) + q_{24}\mathcal{F}_3(s), \\ s^{\xi}\mathcal{F}_3(s) &= q_{31}\mathcal{F}_1(s) + q_{32}\mathcal{F}_2(s) + q_{33}\mathcal{F}_3(s), \end{aligned} \tag{18}$$

in which,

$$\mathcal{F}_1(s) = \mathcal{L}[y_1(t)],\ \mathcal{F}_2(s) = \mathcal{L}[y_2(t)],\ \mathcal{F}_3(s) = \mathcal{L}[y_3(t)].$$

The characteristic matrix $\Delta(s)$ of linear system (17) is

$$\Delta(s) = \begin{pmatrix} s^{\xi} - q_{11} - q_{12}e^{-s\tau} & -q_{13}e^{-s\tau} & -q_{14} \\ -q_{21}e^{-s\tau} & s^{\xi} - q_{22} - q_{23}e^{-s\tau} & -q_{24} \\ -q_{31} & -q_{32} & s^{\xi} - q_{33} \end{pmatrix}.$$

Then the corresponding characteristic equation can be written as

$$A(s) + B(s)e^{-s\tau} + C(s)e^{-2s\tau} = 0. \tag{19}$$

Multiplying $e^{s\tau}$ on both sides of (19), it is easy to get that

$$A(s)e^{s\tau} + B(s) + C(s)e^{-s\tau} = 0, \tag{20}$$

where $A(s) = s^{3\xi} + A_1s^{2\xi} + A_2s^{\xi} + A_3, B(s) = B_1s^{2\xi} + B_2s^{\xi} + B_3, C(s) = C_1s^{\xi} + C_2$, and $A_1 = -(q_{11} + q_{22} + q_{33}), A_2 = q_{22}q_{33} + q_{11}q_{22} + q_{11}q_{33} - q_{24}q_{32} - q_{14}q_{31}, A_3 = -q_{11}q_{22}q_{33} + q_{24}q_{32}q_{11} + q_{14}q_{22}q_{31}, B_1 = -(q_{12} + q_{23}), B_2 = q_{12}q_{22} + q_{12}q_{33} + q_{23}q_{11} + q_{23}q_{33}, B_3 = -q_{12}q_{22}q_{33} - q_{13}q_{24}q_{31} + q_{12}q_{24}q_{32} - q_{23}q_{11}q_{33} - q_{21}q_{32}q_{14} + q_{14}q_{23}q_{31}, C_1 = q_{12}q_{23} - q_{13}q_{21}, C_2 = -q_{12}q_{23}q_{33} + q_{13}q_{21}q_{33}$.
Next, the bifurcation behavior of system (4) will be investigated based on the following analysis.
Assume that $s = i\omega = \omega(\cos\frac{\pi}{2} + i\sin\frac{\pi}{2})(\omega > 0)$ is a purely imaginary root of Equation (20). Then, separating the real and imaginary parts yields:

$$\begin{cases} Re[A(i\omega) + C(i\omega)]\cos(\omega\tau) - Im[A(i\omega) - C(i\omega)]\sin(\omega\tau) = -Re[B(i\omega)], \\ Im[A(i\omega) + C(i\omega)]\cos(\omega\tau) + Re[A(i\omega) - C(i\omega)]\sin(\omega\tau) = -Im[B(i\omega)], \end{cases} \tag{21}$$

where

$$\begin{aligned}
Re[A(i\omega)] &= \omega^{3\xi}\cos\frac{3\pi\xi}{2} + A_1\omega^{2\xi}\cos(\pi\xi) + A_2\omega^{\xi}\cos\frac{\pi\xi}{2} + A_3,\\
Re[B(i\omega)] &= B_1\omega^{2\xi}\cos(\pi\xi) + B_2\omega^{\xi}\cos\frac{\pi\xi}{2} + B_3,\\
Re[C(i\omega)] &= C_1\omega^{\xi}\cos\frac{\pi\xi}{2} + C_2,\\
Im[A(i\omega)] &= \omega^{3\xi}\sin\frac{3\pi\xi}{2} + A_1\omega^{2\xi}\sin(\pi\xi) + A_2\omega^{\xi}\sin\frac{\pi\xi}{2},\\
Im[B(i\omega)] &= B_1\omega^{2\xi}\sin(\pi\xi) + B_2\omega^{\xi}\sin\frac{\pi\xi}{2},\\
Im[C(i\omega)] &= C_1\omega^{\xi}\sin\frac{\pi\xi}{2}.
\end{aligned}$$

Solving Equation (21) yields the following solution:

$$\begin{aligned}
g_1(\omega) = \cos(\omega\tau) &= -\frac{T_3T_5 + T_2T_6}{T_1T_5 + T_2T_4},\\
g_2(\omega) = \sin(\omega\tau) &= \frac{T_3T_4 - T_1T_6}{T_1T_5 + T_2T_4},
\end{aligned} \tag{22}$$

where

$$\begin{aligned}
&T_1 = Re[A(i\omega) + C(i\omega)], T_2 = Im[A(i\omega) - C(i\omega)], T_3 = Re[B(i\omega)],\\
&T_4 = Im[A(i\omega) + C(i\omega)], T_5 = Re[A(i\omega) - C(i\omega)], T_6 = Im[B(i\omega)].
\end{aligned}$$

From (22), we obtain

$$g_1^2(\omega) + g_2^2(\omega) = 1. \tag{23}$$

Assume that Equation (23) has r positive real roots $\omega_j, j = 1, 2, \cdots, r$. Then we obtain

$$\tau_j^{(k)} = \frac{1}{w_j}[\arccos\phi_1(\omega_j) + 2k\pi], k = 0, 1, 2, \cdots, j = 1, 2, \cdots, r. \tag{24}$$

The bifurcation point is defined as

$$\tau_0 = \min\{\tau_j^{(k)}\}, k = 0, 1, 2, \cdots, j = 1, 2, \cdots, r. \tag{25}$$

To derive the condition for the occurrence of Hopf bifurcation, we introduce the following assumption.

(H4): $M_1N_1 + M_2N_2 > 0$.

Based on the aforementioned analysis and assumption (H4), we present the following result. □

Lemma 4. *If* ***(H4)*** *holds, let* $s(\tau) = \varsigma(\tau) + i\omega(\tau)$ *be the root of Equation* (20) *near* $\tau = \tau_0$ *and satisfies* $\varsigma(\tau_0) = 0, \omega(\tau_0) = \omega_0$. *Then the following transversality condition holds*

$$Re\left[\frac{ds}{d\tau}\right]^{-1}_{s=iw_0,\tau=\tau_0} > 0.$$

Proof. Differentiating both sides of Equation (20) with respect to τ yields:

$$\left(\frac{ds}{d\tau}\right)^{-1} = \frac{A'(s)e^{s\tau} + B'(s) + C'(s)e^{-s\tau}}{C(s)e^{-s\tau}s - A(s)e^{s\tau}s} - \frac{\tau}{s}. \tag{26}$$

Let $s = i\omega_0, \tau = \tau_0$, Equation (26) can be written as

$$\left(\frac{ds}{d\tau}\right)^{-1}_{s=i\omega_0,\tau=\tau_0} = \frac{M_1 + iM_2}{N_1 + iN_2} - \frac{\tau_0}{i\omega_0}, \tag{27}$$

where

$$\begin{aligned}
M_1 &= 3\xi\omega_0^{3\xi-1}\cos(\frac{(3\xi-1)\pi}{2} + \omega_0\tau_0) + 2\xi A_1\omega_0^{2\xi-1}\cos(\frac{(2\xi-1)\pi}{2} + \omega_0\tau_0) \\
&\quad + \xi A_2\omega_0^{\xi-1}\cos(\frac{(\xi-1)\pi}{2} + \omega_0\tau_0) + 2\xi B_1\omega_0^{2\xi-1}\cos(\frac{(2\xi-1)\pi}{2} \\
&\quad + \xi B_2\omega_0^{\xi-1}\cos(\frac{(\xi-1)\pi}{2} + \xi C_1\omega_0^{\xi-1}\cos(\frac{(\xi-1)\pi}{2} - \omega_0\tau_0), \\
N_1 &= C_1\omega_0^{\xi+1}\cos(\frac{(\xi+1)\pi}{2} - \omega_0\tau_0) + C_2\cos(\frac{\pi}{2} - \omega_0\tau_0) \\
&\quad + \omega_0^{3\xi+1}\cos(\frac{(3\xi+1)\pi}{2} + \omega_0\tau_0) + A_1\omega_0^{2\xi+1}\cos(\frac{(2\xi+1)\pi}{2} + \omega_0\tau_0) \\
&\quad + A_2\omega_0^{\xi+1}\cos(\frac{(\xi+1)\pi}{2} + \omega_0\tau_0) + A_3\omega_0\cos(\frac{\pi}{2} + \omega_0\tau_0), \\
M_2 &= 3\xi\omega_0^{3\xi-1}\sin(\frac{(3\xi-1)\pi}{2} + \omega_0\tau_0) + 2\xi A_1\omega_0^{2\xi-1}\sin(\frac{(2\xi-1)\pi}{2} + \omega_0\tau_0) \\
&\quad + \xi A_2\omega_0^{\xi-1}\sin(\frac{(\xi-1)\pi}{2} + \omega_0\tau_0) + 2\xi B_1\omega_0^{2\xi-1}\sin(\frac{(2\xi-1)\pi}{2} \\
&\quad + \xi B_2\omega_0^{\xi-1}\sin(\frac{(\xi-1)\pi}{2} + \xi C_1\omega_0^{\xi-1}\sin(\frac{(\xi-1)\pi}{2} - \omega_0\tau_0), \\
N_2 &= C_1\omega_0^{\xi+1}\sin(\frac{(\xi+1)\pi}{2} - \omega_0\tau_0) + C_2\sin(\frac{\pi}{2} - \omega_0\tau_0) \\
&\quad + \omega_0^{3\xi+1}\sin(\frac{(3\xi+1)\pi}{2} + \omega_0\tau_0) + A_1\omega_0^{2\xi+1}\sin(\frac{(2\xi+1)\pi}{2} + \omega_0\tau_0) \\
&\quad + A_2\omega_0^{\xi+1}\sin(\frac{(\xi+1)\pi}{2} + \omega_0\tau_0) + A_3\omega_0\sin(\frac{\pi}{2} + \omega_0\tau_0).
\end{aligned}$$

Then it is easy to see

$$Re\left[\frac{ds}{d\tau}\right]^{-1}_{s=iw_0,\tau=\tau_0} = \frac{M_1N_1 + M_2N_2}{N_1^2 + N_2^2} > 0.$$

Based on the aforementioned discussions and the two lemmas, we draw the following conclusion. □

Theorem 6. *Assume that **(H4)** holds. Then the following results about system (4) are established:*

(i) The equilibrium point E_3 is locally asymptotically stable for $\tau \in (0, \tau_0)$.
(ii) For $\tau > \tau_0$, the equilibrium point E_3 of system (4) is unstable.
(iii) System (4) undergoes a Hopf bifurcation at E_3 when $\tau = \tau_0$.

7. Numerical Simulations

In this section, we aim to validate the theoretical analyses presented in the preceding sections and elucidate the combined effects of fractional order and time delay on the stability of system (4).

Consider the following parameters:

$$r_1 = 1.8, a_1 = 0.32, b_1 = 1.8, c_1 = 0.4, \varphi_1 = 0.35, r_2 = 1.4, a_2 = 0.28,$$

$$b_2 = 2.0, c_2 = 0.35, \varphi_2 = 0.45, r_3 = 0.3, a_3 = 0.7, \varphi_3 = 0.25, \varphi_4 = 0.15.$$

By performing a direct calclation, we find that (H1–H4) are satisfied for the given parameters. In addition, for $r_3, a_3, \varphi_3, \varphi_4 > 0$, we confirm the coexistence of the equilibrium

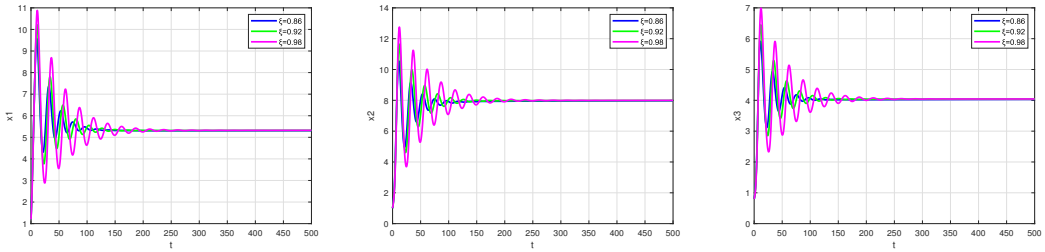
point using both analytical and numerical approaches. By further calculation, we obtain a positive equilibrium point:

$$E_3 = (5.318, 7.988, 4.039).$$

In addition, the initial values are taken as $x_1(0) = 1.2, x_2(0) = 1.0, x_3(0) = 0.8$.

Example 1. *Influence of memory parameter ξ on the dynamical behaviour of the system (4).*

We assume $\tau = 0$. Figure 2a–c presents the time series of solutions for system (4) under three distinct values of the fractional order ξ. A smaller ξ results in enhanced stability and a faster convergence rate, whereas a larger ξ induces more intense oscillations and a slower convergence rate. Since a smaller ξ denotes stronger memory effects, these findings indicate that an increase in memory effects contributes to a wider stability region of the system. This phenomenon is rooted in the memory mechanism of the Caputo fractional derivative and the characteristic root stability criterion (Lemma 1). Physically, $\xi \in (0, 1)$ measures the system's nonlocal time memory intensity: a smaller ξ implies stronger global memory that integrates historical dynamical information, acting as a regularization term to suppress perturbation amplification and damp oscillations. Mathematically, the stability condition $|\arg(\lambda_i)| > \frac{\xi\pi}{2}$ means a smaller ξ narrows the unstable root sector in the complex plane and expands the stable root domain. This directly enlarges the stability region in the parameter space and boosts the system's perturbation robustness, consistent with the numerical results in Figure 2.

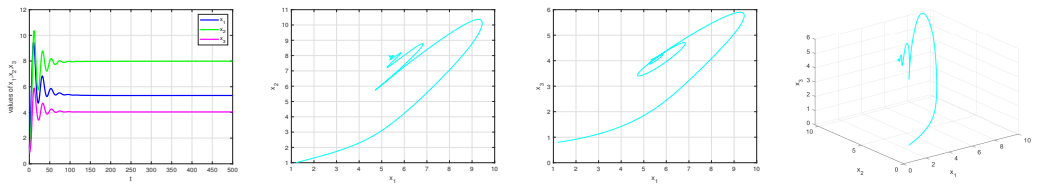


(**a**) (**b**) (**c**)

Figure 2. Time series diagram of $x_1(t), x_2(t)$, and $x_3(t)$ of system (4) at E_3 with $\tau = 0$ when $\xi = 0.86,\ 0.92,\ 0.98$, where (**a**) denotes the time series diagram of $x_1(t)$; (**b**) denotes the time series diagram of $x_2(t)$; (**c**) denotes the time series diagram of $x_3(t)$.

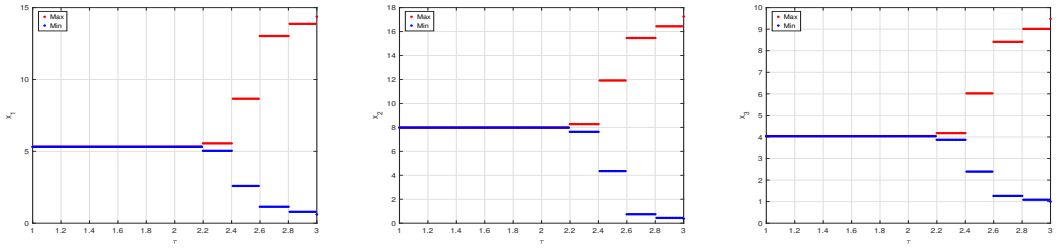
Example 2. *The impact of time delays on the stability and Hopf bifurcation of the system (4).*

Under the parameter values $\xi = 0.90$ and $\tau = 0$, the system dynamics are locally asymptotically stable at equilibrium E_3, as shown in Figure 3. Furthermore, we consider τ as a bifurcation parameter. For $\xi = 0.90$ and with the other parameters are same as above, the critical bifurcation value $\tau_0 = 2.05$ is calculated from Equations (23) and (24). The corresponding bifurcation diagram for the parameter τ is shown in Figure 4a–c.



(**a**) (**b**) (**c**) (**d**)

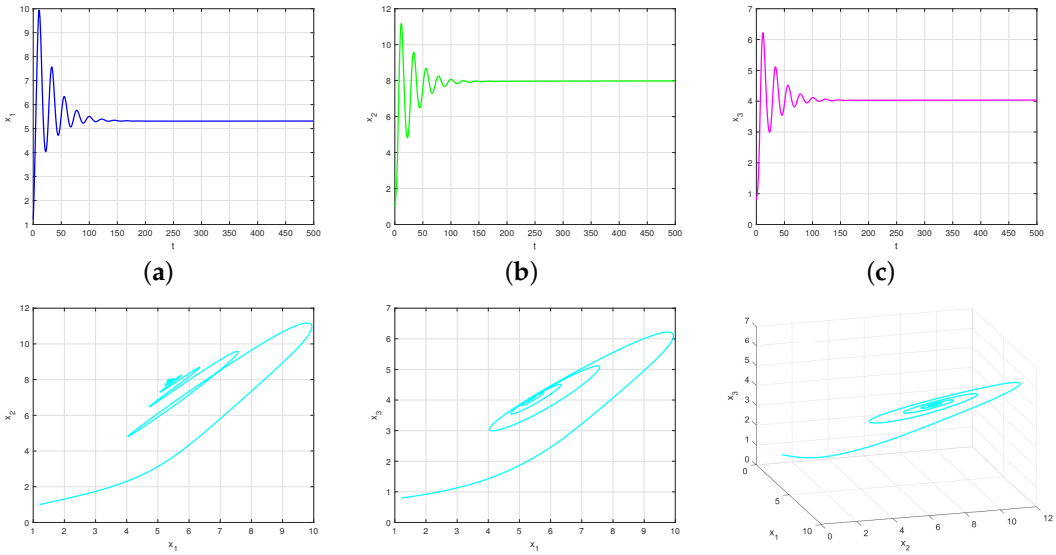
Figure 3. Local asymptotic stability diagram of system (4) at E_3 with $\xi = 0.90$ and $\tau = 0$, where (**a**) denotes the stable time series diagram of $x_1(t), x_2(t)$, and $x_3(t)$; (**b**) denotes the stable planar phase diagram of $x_1(t), x_2(t)$; (**c**) denotes the stable planar phase diagram of $x_1(t), x_3(t)$; (**d**) denotes the stable space phase diagram of $x_1(t), x_2(t), x_3(t)$.



(**a**) (**b**) (**c**)

Figure 4. Bifurcation phase diagram of system (4) with respect to the time delay τ when $\xi = 0.90$. In (**a**–**c**), the Hopf bifurcation occurs at the critical point $\tau_0 = 2.05$.

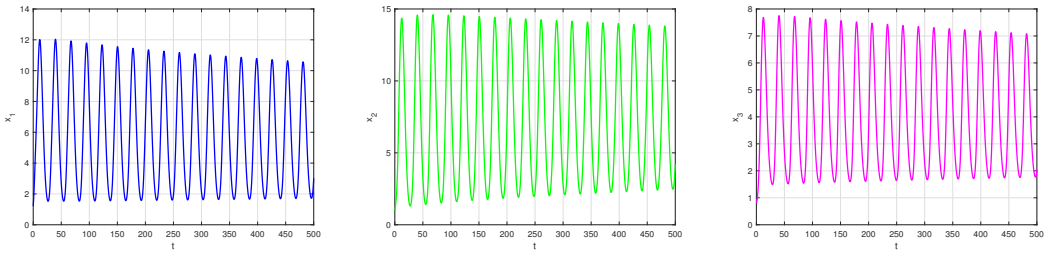
Numerical analysis for $\xi = 0.90$ yields a critical delay $\tau_0 = 2.05$. It is easy to confirm that (H4) holds. From Theorem 5, the equilibrium point $E_3 = (5.318, 7.988, 4.039)$ is asymptotically stable when the time delay $\tau = 1.95 < \tau_0$, as numerically demonstrated in Figure 5a–f. Conversely, when $\tau = 2.25 > \tau_0$, the equilibrium $E_3 = (5.318, 7.988, 4.039)$ becomes unstable and a Hopf bifurcation occurs, which is illustrated in Figure 6a–f.



(**a**) (**b**) (**c**)

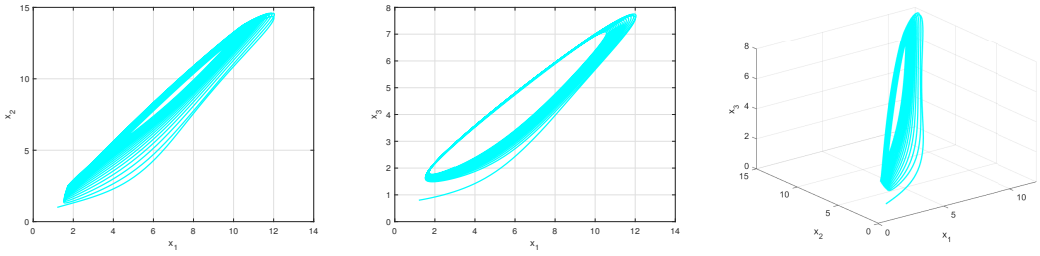
(**d**) (**e**) (**f**)

Figure 5. Time series and phase diagram of $x_1(t), x_2(t)$ and $x_3(t)$ when $\xi = 0.90, \tau = 1.95$. Panels (**a**–**f**) show the stable phase diagrams of $x_1(t)$, $x_2(t)$, and $x_3(t)$ for $\xi = 0.90$ and $\tau = 1.95$.



(**a**) (**b**) (**c**)

Figure 6. *Cont.*



(**d**) (**e**) (**f**)

Figure 6. Time series and phase diagram of $x_1(t), x_2(t)$ and $x_3(t)$ when $\xi = 0.90, \tau = 2.25$. Panels (**a**–**f**) show the unstable phase diagrams of $x_1(t)$, $x_2(t)$, and $x_3(t)$ for $\xi = 0.90$ and $\tau = 2.25$.

8. Conclusions

This study examines a fractional-order Lotka–Volterra system with delay that incorporates both competitive and cooperative interactions. First, we prove the boundedness and uniqueness of the solutions. Through numerical simulations, we systematically explain the influence of the delay τ and fractional order ξ on the stability and bifurcation behavior of the system. When the delay exceeds the critical threshold τ_0, the system undergoes a Hopf bifurcation and produces periodic oscillations. Notably, compared with the integer-order system, the fractional-order system exhibits a wider stability region when the order ξ is appropriately reduced, which mainly results from its inherent memory-dependent properties.

In-depth comparison with integer-order ($\xi = 1$) competitive–competitive–cooperative systems [12,13] and Holling type II functional response systems [42] reveals distinct dynamical advantages of our model: integer-order systems have a narrower stability region and smaller critical τ_0, while our fractional-order system exhibits a wider stability region and damped oscillation characteristics after bifurcation; the B-D response avoids the unrealistic infinite growth of Holling type II at high species densities, and its interference terms weaken interspecific competition to further enhance system stability.

In addition, the combination of fractional order $\xi = 1$, delay τ and B-D response introduces three unique dynamical features: (1) $\xi = 1$ acts as a stability regulator for delay-induced Hopf bifurcation, with a smaller $\xi = 1$ increasing τ_0 and compensating for delays destabilizing effect; (2) B-D interference terms nonlinearly modulate the memory effect of $\xi = 1$ and the sensitivity of the system to $\xi = 1$; (3) the amplitude and frequency of post-bifurcation oscillations are jointly determined by $\xi = 1$, τ and B-D parameters, differing from the fixed oscillatory features in integer-order Holling II systems [42].

Although this study establishes a theoretical framework for system stability and bifurcation, several limitations require further investigation. First, the treatment of the time delay in the model is relatively idealized and does not consider the multiple delay effects that may exist in different ecological processes. Second, this research primarily focuses on competitive and cooperative interactions, whereas real ecosystems often involve more complex coexistence of multiple interaction types. Therefore, future research will focus on developing a theoretical framework for multi-delay dynamics, analyzing the dynamic patterns of coupled ecological interactions, and investigating the stability and bifurcation behavior of fractional-order stochastic systems.

Author Contributions: Conceptualization, T.Z. and A.M.; methodology, T.Z.; software, T.Z.; validation, T.Z. and A.M.; formal analysis, T.Z. and A.M.; writing—original draft preparation, T.Z. and A.M.; writing—review and editing, T.Z. and A.M.; supervision, A.M. All authors have read and agreed to the published version of the manuscript.

Funding: This research is supported by the National Natural Science Foundation of Xinjiang (grant no. 2025D01C41), the National Natural Science Foundation of China (12461097) and the Open Project of Xinjiang Key Laboratory of Applied Mathematics (grant no. 2023D04045).

Data Availability Statement: There is no data associated with this paper.

Conflicts of Interest: The authors declare that they have no competing interests.

References

1. Lotka, A.J. *Elements of Physical Biology*; Williams Wilkins: Philadelphia, PA, USA, 1925.
2. Volterra, V. Fluctuations in the abundance of a species considered mathematically. *Nature* **1926**, *118*, 558–560. [CrossRef]
3. Khajanchi, S.; Banerjee, S. Role of constant prey refuge on stage structure predator-prey model with ratio dependent functional response. *Appl. Math. Comput.* **2017**, *314*, 193–198. [CrossRef]
4. Shang, Z.; Qiao, Y. Multiple bifurcations in a predator-prey system of modified Holling and Leslie type with double Allee effect and nonlinear harvesting. *Math. Comput. Simul.* **2023**, *205*, 745–764. [CrossRef]
5. Li, H.; Tian, Y. Dynamic behavior analysis of a feedback control predator-prey model with exponential fear effect and Hassell-Varley functional response. *J. Frankl. Inst.* **2023**, *360*, 3479–3498. [CrossRef]
6. Sasmal, S.K.; Takeuchi, Y. Modeling the Allee effects induced by cost of predation fear and its carry-over effects. *J. Math. Anal. Appl.* **2022**, *505*, 125485. [CrossRef]
7. Balci, E. Predation fear and its carry-over effect in a fractional order prey-predator model with prey refuge. *Chaos Solitons Fractals* **2023**, *175*, 114016. [CrossRef]
8. Zhang, Z. Mutualism or cooperation among competitors promotes coexistence and competitive ability. *Ecol. Model.* **2003**, *164*, 271–282. [CrossRef]
9. Kundu, S.; Maitra, S. Dynamical behaviour of a delayed three species predator-prey model with cooperation among the prey species. *Nonlinear Dyn.* **2018**, *92*, 627–643. [CrossRef]
10. Xu, C.J.; Liao, M.X.; Li, P.L. Bifurcation control of a fractional-order delayed competition and cooperation model of two enterprises. *Sci. China Technol. Sci.* **2019**, *62*, 2130–2143. [CrossRef]
11. Cai, Y.; Liu, P.; Li, Y. Persistence analysis of a three-species predation-competition discrete time-delay model with feedback control and nonlinear inhibition in the effects of toxicants. *J. Yunnan Univ. Nat. Sci. Ed.* **2022**, *44*, 435–443.
12. Lv, X.; Yan, P.; Lu, S. Existence and global attractivity of positive periodic solutions of competitor-competitor-mutualist Lotka-Volterra systems with deviating arguments. *Math. Comput. Model.* **2010**, *51*, 823–832. [CrossRef]
13. Wang, C.; Li, L.; Zhang, Q.; Li, R. Dynamical behaviour of a Lotka-Volterra competitive-competitive-cooperative model with feedback controls and time delays. *J. Biol. Dyn.* **2019**, *13*, 43–68. [CrossRef] [PubMed]
14. Muhammadhaji, A.; Halik, A.; Li, H.L. Dynamics in a ratio-dependent Lotka-Volterra competitive-competitive-cooperative system with feedback controls and delays. *Adv. Differ. Equ.* **2021**, *2021*, 230. [CrossRef]
15. Huang, C.; Zhang, H.; Cao, J.; Hu, H. Stability and Hopf bifurcation of a delayed prey-predator model with disease in the predator. *Int. J. Bifurc. Chaos* **2019**, *29*, 1950091. [CrossRef]
16. Ojha, A.; Thakur, N.K. Exploring the complexity and chaotic behavior in plankton-fish system with mutual interference and time delay. *BioSystems* **2020**, *198*, 104283. [CrossRef]
17. Parwaliya, A.; Singh, A.; Kumar, A.; Barman, D. The impact of delays on prey-predator dynamics with predation-induced fear. *J. Appl. Math. Comput.* **2024**, *70*, 4877–4907. [CrossRef]
18. Chang, L.; Sun, G.Q.; Wang, Z.; Jin, Z. Rich dynamics in a spatial predator-prey model with delay. *Appl. Math. Comput.* **2015**, *256*, 540–550. [CrossRef]
19. Hanif, H. A computational approach for boundary layer flow and heat transfer of fractional Maxwell fluid. *Math. Comput. Simul.* **2022**, *191*, 1–13. [CrossRef]
20. Vellappandi, M.; Lee, S. Physics-informed neural fractional differential equations. *Appl. Math. Model.* **2025**, *145*, 116127. [CrossRef]
21. Wang, W.; Ralescu, D.A.; Zhang, P. Valuation of convertible bond based on uncertain fractional differential equation. *Fuzzy Optim. Decis. Mak.* **2024**, *23*, 513–538. [CrossRef]
22. Xin, Y.; Zhang, Y.; Noorani, I.; Mehrdoust, F.; Gao, J. Estimation of parameters and valuation of options written on multiple assets described by uncertain fractional differential equations. *Appl. Math. Comput.* **2025**, *487*, 129109. [CrossRef]
23. Xu, C.; Aouiti, C.; Liu, Z.; Li, P.; Yao, L. Bifurcation caused by delay in a fractional-order coupled oregonator model in chemistry. *MATCH Commun. Math. Comput. Chem.* **2022**, *88*, 371–396. [CrossRef]
24. Zeng, J.; Chen, X.; Wei, L.; Li, D. Bifurcation analysis of a fractional-order eco-epidemiological system with two delays. *Nonlinear Dyn.* **2024**, *112*, 22505–22527. [CrossRef]
25. Kumar, A.; Kumar, S.; Momani, S.; Hadid, S. A chaos study of fractal-fractional predator-prey model of mathematical ecology. *Math. Comput. Simul.* **2024**, *225*, 857–888. [CrossRef]

26. Pang, X.; Qiao, Y. Bifurcation and chaos in a multi-trophic eco-epidemiological model with fear effect and nonlinear functional responses. *Chaos Solitons Fractals* **2025**, *200*, 116987. [CrossRef]
27. Ali, I. Dynamical behavior of stochastic fractional-order predator-prey system with nonlinear functional response and Allee effect: I. Ali. *J. Appl. Math. Comput.* **2025**, *71*, 4043–4065. [CrossRef]
28. Rihan, F.A.; Rajivganthi, C. Dynamics of fractional-order delay differential model of prey-predator system with Holling-type III and infection among predators. *Chaos Solitons Fractals* **2020**, *141*, 110365. [CrossRef]
29. Liu, J.; Wei, W.; Wang, J.; Xu, W. Limit behavior of the solution of Caputo-Hadamard fractional stochastic differential equations. *Appl. Math. Lett.* **2023**, *140*, 108586. [CrossRef]
30. Berkal, M.; Navarro, J.F.; Hamada, M.Y.; Semmar, B. Qualitative behavior for a discretized conformable fractional-order predator-prey model. *J. Appl. Math. Comput.* **2025**, *71*, 4815–4837. [CrossRef]
31. Chen, S.; Lou, Y.; Wei, J. Hopf bifurcation in a delayed reaction-diffusion-advection population model. *J. Differ. Equ.* **2018**, *264*, 5333–5359. [CrossRef]
32. Ma, Y.; Yang, R. Hopf-Hopf bifurcation in a predator-prey model with nonlocal competition and refuge in prey. *Discret. Contin. Dyn. Syst.-B* **2024**, *29*, 2582–2609. [CrossRef]
33. Lv, Y. Influence of predator-taxis and time delay on the dynamical behavior of a predator-prey model with prey refuge and predator harvesting. *Chaos Solitons Fractals* **2025**, *196*, 116388. [CrossRef]
34. Huang, C.; Wang, H.; Cao, J.; Liu, H. Delay-dependent bifurcation conditions in a fractional-order inertial BAM neural network. *Chaos Solitons Fractals* **2024**, *185*, 115106. [CrossRef]
35. Li, P.; Gao, R.; Xu, C.; Ahmad, S.; Li, Y.; Akgül, A. Bifurcation behavior and PD control mechanism of a fractional delayed genetic regulatory model. *Chaos Solitons Fractals* **2023**, *168*, 113219. [CrossRef]
36. Zhang, H.; Muhammadhaji, A. A delayed fractional-order predator-prey model with three-stage structure and cannibalism for prey. *Fractal Fract.* **2024**, *8*, 492. [CrossRef]
37. Zhang, H.; Muhammadhaji, A. Dynamics of a delayed fractional-order predator-prey model with cannibalism and disease in prey. *Fractal Fract.* **2024**, *8*, 333. [CrossRef]
38. Li, H.L.; Zhang, L.; Hu, C.; Jiang, Y.L.; Teng, Z. Dynamical analysis of a fractional-order predator-prey model incorporating a prey refuge. *J. Appl. Math. Comput.* **2017**, *54*, 435–449. [CrossRef]
39. Niu, Y.; Muhammadhaji, A. Dynamics of a fractional-order IDSR rumor propagation model with time delays. *Fractal Fract.* **2025**, *9*, 242. [CrossRef]
40. Krasnoselskii, M.A. *Positive Solutions of Operator Equations*; Noordhoff: Groningen, The Netherlands, 1964.
41. Cox, D.A.; Little, J.; O'Shea, D. *Using Algebraic Geometry*; Springer: Berlin/Heidelberg, Germany, 2005.
42. Damag, F.H.; Qurtam, A.A.; Almalahi, M.; Aldwoah, K.; Adel, M.; Abd El-Latif, A.M.; Hassan, E.I. A comparative analysis of harmonic mean, Holling type II, Beddington-DeAngelis, and Crowley-Martin incidence rates of a piecewise dengue fever dynamics model. *Fractal Fract.* **2025**, *9*, 400. [CrossRef]

Disclaimer/Publisher's Note: The statements, opinions and data contained in all publications are solely those of the individual author(s) and contributor(s) and not of MDPI and/or the editor(s). MDPI and/or the editor(s) disclaim responsibility for any injury to people or property resulting from any ideas, methods, instructions or products referred to in the content.